Sterically Induced Conformational Relaxation and Structure of meso −Diaryloctaalkyl Porphyrins in the Excited Triplet State: Experimental and DFT Studies

4 AUTHORS:

Alexander Kyrychenko
V. N. Karazin Kharkiv National University
66 PUBLICATIONS 877 CITATIONS

SEE PROFILE

Joakim Andreasson
Chalmers University of Technology
58 PUBLICATIONS 2,343 CITATIONS

SEE PROFILE

Jerker Mårtensson
Chalmers University of Technology
58 PUBLICATIONS 1,769 CITATIONS

SEE PROFILE

Bo Albinsson
Chalmers University of Technology
135 PUBLICATIONS 4,594 CITATIONS

SEE PROFILE

Sterically Induced Conformational Relaxation and Structure of *meso*-Diaryloctaalkyl Porphyrins in the Excited Triplet State: Experimental and DFT Studies

Alexander Kyrychenko,[†,‡] Joakim Andréasson,[†] Jerker Mårtensson,[§] and Bo Albinsson*,[†]

Department of Physical Chemistry and Department of Organic Chemistry, Chalmers University of Technology, SE-412 96 Göteborg, Sweden

Received: June 14, 2002; In Final Form: September 11, 2002

The excited triplet state conformations of zinc and free base 5,15-diaryloctaalkylporhyrins are studied by experimental and computational (density functional theory, DFT) methods. From the observations of an unusual triplet state dynamics, i.e., fast nonradiative and biexponential decay, it has been suggested that these porphyrins exist in two distinguishable conformers in the lowest excited triplet state. X-ray crystallography and DFT (B3LYP/6-31G(d)) optimization of the ground state show that the porphyrins are planar prior to excitation. However, in the excited triplet state, the planar structure relaxes to an out-of-plane distorted saddle-shaped conformer. This distorted conformer and the lowest triplet potential energy surface are characterized by DFT calculations. It is suggested that the conformational relaxation explains the unusual triplet dynamics of this class of porphyrins.

Introduction

Conformationally distorted porphyrins have been investigated intensively since discovering the importance of tetrapyrrole macrocycle nonplanarity for biological functions.[1] Collection and transport of light energy in antennae complexes, conversion of solar energy to chemical energy in photosynthetic reaction centers, and electron transfer in cytochromes have all been suggested to be highly sensitive to the conformational properties of porphyrin chromophores.[2] The nonplanarity of porphyrins in biological systems is currently believed to be induced by external forces of surrounding proteins.[3] However, the skeletal distortions of the tetrapyrrole macrocycle can be imposed, in a controllable way, by peripheral substituents.[4–9] The flexibility of the tetrapyrrole macrocycle was demonstrated in an essential body of the available X-ray data.[4,10–12] It has also been shown that metallooctaalkylporphyrins in solution coexist in an equilibrium of multiple nonplanar macrocycle conformations.[13] The flexibility of octaalkylporphyrins has revealed a selective sensitivity for the atomic size of the metal ion, located in the macrocycle cavity.[14] Metal ions with a small atomic size, such as nickel(II), are expected to cause nonplanar macrocycle distortions.[15] The ability to reach the stronger metal–N bonding due to the shorter bond lengths, achieved in a nonplanar macrocycle conformation, has been suggested to be the main driving force for this kind of structural distortion.[14,16] Larger metal ions, such as zinc(II), appear to force a planar macrocycle of octaalkylporphyrins to be energetically favorable.[15] It has also been shown that further introduction of aryl groups to the meso positions of an octaalkyl-substituted macrocycle can cause dramatic changes of the porphyrin skeleton planarity.[4–8,10,11] In this case, the metal size effect is weak and suppressed by sterical effects of the peripheral groups. Thus, an essential body of experimental evidences provides the basis for speculation that an originally energetically favorable planar macrocycle conformation is able to be significantly perturbed by internal (structural modifications[4,5,16,17]) and external (ligation[13–15] or solvent[5]) stimuli and undergoes structural distortions as a result of a balance between competitive electronic and steric effects. The equilibrium geometry of sterically crowded porphyrins can also be destabilized and significantly altered in response to external perturbation such as photoexcitation.[4,5,13,17–19]

In liquid solution, interconversion between accessible conformations, separated by relatively small energy barriers, involves out-of-plane macrocycle distortions and motions of peripheral substituents. As a result, absorption and emission bands of conformationally flexible porphyrins are usually red-shifted and broadened as compared to those of their planar analogues.[5,16–18,20] Upon photoexcitation, the energy preference of different conformations can be changed, or even reversed, and a new equilibrium geometry might be reached according to the excited state electronic density distribution. Such an excited state conformational relaxation can cause pronounced structural changes in the peripherally crowded porphyrins.[8,16–19] In this case, the displacement of the excited relative to the ground state surface can be significant.[5,8,16–19] The excited state lifetime of such porphyrins is usually dramatically shortened and is often found to be multiexponential. Conformational interconversion is able to access some parts of an excited state surface characterized by a smaller energy gap to the ground state and by more favorable Franck–Condon factors for rapid nonradiative deactivation, which is believed to be responsible for the observed "unusual photophysics".[5,8,9,16–19,21] In rigid organic glasses at low temperature where the conformational freedom is restricted, the photophysics typical for the "normal" class of porphyrins is restored.[5,9,16,21]
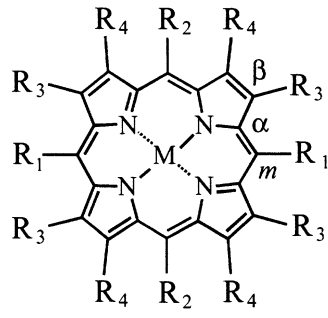
Recently, several studies on resonance Raman spectroscopy of porphyrins[22–30] in electronically excited states have appeared. The investigation of the number and symmetry of the bands has shown that the nature of structural changes accompanying formation of the S_1 and T_1 states is different.[23,26] It has been suggested that the partial occupation of the degenerate or

* To whom correspondence should be addressed. Tel: 46-31-772 30 44. Fax: 46-31-772 38 58. E-mail: balb@phc.chalmers.se.
  † Department of Physical Chemistry, Chalmers University of Technology.
  ‡ Permanent address: Research Institute for Chemistry, Kharkov State University, 4, Svobody Square, 310077 Kharkov, Ukraine.
  § Department of Organic Chemistry, Chalmers University of Technology.

12614 *J. Phys. Chem. B, Vol. 106, No. 48, 2002*

Kyrychenko et al.

CHART 1: Formulas and Acronyms of Reference and Model Porphyrins

	M	R_1	R_2	R_3	R_4	
ZnP	Zn	H	H	H	H	
H_2P	2H	H	H	H	H	
ZnOMP	Zn	H	H	-CH_3	-CH_3	
H_2OMP	2H	H	H	-CH_3	-CH_3	
ZnOEP	Zn	H	H	-CH_2CH_3	-CH_2CH_3	Reference
H_2OEP	2H	H	H	-CH_2CH_3	-CH_2CH_3	porphyrins
ZnTPP	Zn	Ph	Ph	H	H	
H_2TPP	2H	Ph	Ph	H	H	
H_2DAOAP	2H	Ar*	H	-CH_3	-CH_2CH_3	
ZnDPOMP	Zn	Ph	H	-CH_3	-CH_3	Model
H_2DPOMP	2H	Ph	H	-CH_3	-CH_3	porphyrins

* 3,5-di-*tert*-butylphenyl

Figure 1. Schematic ground and excited state potential energy surfaces and corresponding photophysical processes accompanying the conformational relaxation in the lowest triplet state.

pseudo-degenerate lowest unoccupied molecular orbitals (LUMO) orbitals of the high symmetry porphyrins in their electronically excited state appears to make them potentially active as objects for Jahn−Teller (J−T) distortions,[22,23,26,30] which are expected to exhibit different qualitative effects for the excited states of different spin multiplicity.[23,26,30,31] The J−T effect provides the basis for speculations that porphyrins such as ZnTPP or H_2-TPP (Chart 1), which are treated as normal in terms of the triplet state decay, at the same time reveal significant structural alterations specific for the excited triplet states. Prendergast and Spiro carried out a MNDO/3 study[32] on the lowest excited triplet state of ZnP and found the symmetry breaking of the porphyrin core to be related to the J−T effect, and further, to be accompanied by a striking bond length alternation. Thus, the J−T distortions can potentially account for different flexibility of the porphyrin skeleton in the S_0 and T_1 states.

   The available information regarding the spectral properties of conformationally distorted porphyrins has often been restricted to the cases where the "unusual" effects are simultaneously observed in both the ground and the excited states. Thus, to some extent, the unusual excited state behavior is already predetermined in the ground state. Recently, another interesting class of porphyrins, representing an intermediate case between highly substituted nonplanar and planar porphyrins, has been studied.[33−35] The S_0 and S_1 state properties of these *meso*-diaryloctaalkylporphyrins (DAOAP) have been found to be similar to normal planar porphyrins. However, the lifetime of the lowest excited triplet state is dramatically shortened. Conformational changes of the porphyrin macrocycle in the T_1 state have been suggested to be the most probable reason for the unusual photophysics of this class of porphyrins (Figure 1). Detailed studies on the decay kinetics of the T_1 state have allowed us to detect two different triplet species, called T_{1A} and T_{1B}, where the T_{1A} species is structurally similar to the ground state conformation (planar) and the T_{1B} species is structurally distorted. Interconversion of the T_{1A} state into T_{1B} follows a "mother−daughter" relationship, and the overall decay depends strongly on temperature. Evidence that such conformational interconversions can cause unusual triplet photophysics
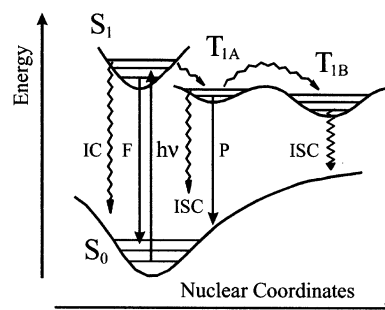
has also been reported for more sterically crowded porphyrins (e.g., 2,3,7,8,12,13,17,18-octaalkyl-5,10,15,20-tetraphenylporphyrins).[36,37] However, a similar conformational behavior is observed for these porphyrins in both the S_0 and the S_1 states. Thus, the occurrence of the conformation dynamics in the T_1 state in this case is not specific for a certain electronic state and originates rather from the ground state conformational heterogeneity. The *meso*-diaryloctaalkylporphyrins represent a particular class of porphyrins for which the equilibrium T_1 geometry differs substantially from those of the S_0 and S_1 states.

   This unusual triplet state dynamics motivated us to study the solvent viscosity dependence of the transformation process because the $T_{1A} \rightarrow T_{1B}$ conformational relaxation is expected to involve high amplitude motions of the bulk meso-aryl substituents and alkyl groups, and these motions are potentially sensitive to solvent viscosity.
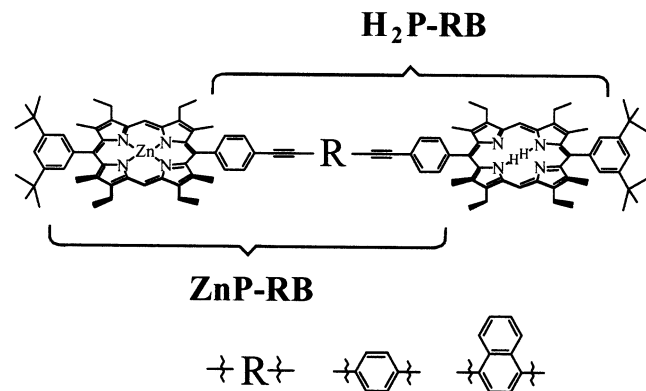
   Although the existence of conformationally distorted porphyrins in electronically excited states has been spectroscopically detected, detailed information for their structures is still a difficult task even for simple porphyrins. Recent successes with employing quantum chemical methods for accurate prediction of an electronic structure of porphyrins in the S_0[38−41] and T_1[42−45] states have encouraged us to carry out a density functional theory-based (DFT) study of the potential energy surface and the energetics for series of free base and zinc(II) *meso*-diphenyloctamethylporphyrins. The primary goal is to determine the geometry and possible conformations of H_2DPOMP and ZnDAOMP (Chart 1) in both the S_0 and the T_1 states. On the basis of this knowledge, we will discuss how the energy gap between the ground and the lowest triplet states is affected by conformational distortions of the porphyrin macrocycle and how this, in turn, influences the photophysics of this group of porphyrins.

Experimental and Computational Details

   Materials. The synthesis and purification of the compounds are described elsewhere.[46,47] The structures of all experimentally studied compounds are shown in Chart 2. The spectroscopic measurements were performed with either 2-methyltetrahydrofuran (MTHF, purchased from ACROS), a 1:6 mixture (v/v) of toluene/methylcyclohexane (toluene/MCH, purchased from LABSCAN and MERCK, respectively), a 1:1 mixture (w/w) of toluene/polystyrene (toluene/PS), or PS films as the solvent.

   Spectroscopic Measurements. Ground state absorption spectra were recorded using a CARY 4B UV/Vis spectrometer. Triplet lifetimes were determined by laser flash photolysis or by xenon lamp pulsed excitation followed by time-resolved gated phosphorescence detection using a SPEX 1934D3 phosphorimeter. In the flash photolysis experiments, the excitation source was the 532 nm second harmonics of a Nd:YAG laser

Porphyrins in the Excited Triplet State

J. Phys. Chem. B, Vol. 106, No. 48, 2002 **12615**

CHART 2: Structure of the Zinc (ZnP−RB) and Free Base (H₂P−RB) Porphyrin Subunits Studied in This Paper
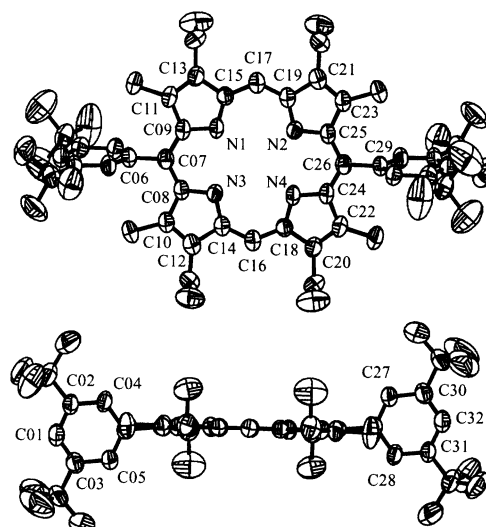

Figure 2. Two views of the crystal structure and labeling scheme for H₂DAOAP. Ellipsoids are drawn for 50% occupancy. Hydrogen atoms have been omitted for clarity.

(Spectron Laser Systems SL803G1270). The monitoring system consisted of a pulsed xenon lamp followed by a conventional monochromator photomultiplier system (symmetrical Czerny− Turner arrangement and a five stage Hamamatsu R928). Data acquisition was performed via a Philips model PM 3323 digital oscilloscope. To minimize interference from triplet annihilation and self-quenching and to avoid kinetic distortions caused by inhomogeneities in the sample distribution, the ground state absorption at 532 nm was adjusted to 0.05 and the $T_1–T_n$ absorption was kept below 0.15.[48] In the temperature interval in which transient absorption was measured, the triplet lifetime of the compounds studied showed no concentration dependence. This excludes that bimolecular processes limit the triplet lifetimes. Ground state absorption spectra recorded after the transient absorption measurements showed neither significant bleaching nor additional absorption bands. All samples were carefully degassed by six freeze−pump−thaw cycles to a final pressure of ca. 10^{-4} Torr. Low temperature measurements were done in a nitrogen-cooled cryostat (Oxford Instruments) equipped with a temperature regulator. The triplet excitation energies of the different species were estimated from the 0−0 phosphorescence transitions measured at 80 K.

Quantum Chemical Computational Setups. All DFT calculations were performed using the Gaussian 98 (revision A. 9) suite of programs.[49] The S_0 and T_1 state geometries were obtained using Becke's three parameter hybrid functional,[50] referred to as B3LYP, and the 6-31G(d) basis set.[51,52] Open-shell DFT calculations for the triplets were carried out using the unrestricted formalism. The spin contamination $\langle S^2 \rangle$ values for all triplets were below 2.06. The S_0 and T_1 geometries were fully optimized without any symmetry assumptions, and on the next step, the optimization was repeated with the symmetry constraint, depending on the resultant symmetry of the uncon- strained optimization. The optimized structures were verified to correspond to the minima by calculating and diagonalizing the matrix of the second derivatives of energy (Hessian) and establishing that there are no imaginary frequencies. The vertical excitation energies were calculated at the same DFT level using the time-dependent density functional response theory (TD-DFT).[53]

Results and Discussion

This work is a part of an ongoing project on the intramo- lecular bridge-dependent triplet energy transfer in the donor− bridge−acceptor (D−B−A) porphyrin dimers.[54,55] A set of dimers consists of a zinc porphyrin as the energy donor and a free base porphyrin as the energy acceptor, covalently connected

by a rigid bridging chromophore (Chart 2). The free base (H₂P− RB) and zinc(II) 5,15-diaryloctaalkyl (ZnP−RB) porphyrins studied in this work are therefore the subunits of the D−B−A systems.

The experimental section is organized as follows: First, the molecular design and the ground state structure of ZnP−RB and H₂P−RB are described. The ground state absorption and fluorescence spectra are briefly considered. Second, the time-resolved $T_1 \rightarrow T_n$ absorption and the lowest triplet state decay are presented. The conformational relaxation dynamics of ZnP− RB and H₂P−RB in the T_1 state is described in terms of the two state mother−daughter kinetic model.[35] Third, the temper- ature and solvent dependencies of the conformational $T_{1A} \rightarrow T_{1B}$ relaxation process are studied and the activation energies for the excited state relaxation are derived.

In the theoretical section, we have applied the DFT method to study the molecular and electronic structure of a series of reference and model porphyrins (Chart 1). In the simplified models of ZnP−RB and H₂P−RB, the β-ethyl groups were replaced by methyl substituents and the meso-aryl moieties were represented by phenyl groups, i.e., ZnDPOMP and H₂DPOMP. First, we carried out geometry optimization of the reference porphyrins in the S_0 and T_1 states to estimate the reliability of the theory level used. Second, the geometry optimization was repeated for the model porphyrins in the S_0 and T_1 states. The influence of the peripheral substituents is studied in terms of their ability to perturb the porphyrin macrocycle planarity. The conformational changes of the macrocycle from a planar to a saddle-shaped distorted form are examined, and the energetics of the ground and excited triplet state surfaces are considered. Finally, the conformational dynamics in the T_1 state are discussed in terms of the efficiency for nonradiative decay and how it depends on the energy gap between the S_0 and the T_1 surfaces.

X-ray Structure. The experimentally determined crystal structure of 5,15-bis(3,5-di-*tert*-butylphenyl)-2,8,12,18-tetra- ethyl-3,7,13,17-tetramethyl free base porphyrin (H₂DAOAP) is shown in Figure 2. The structure is characterized by a nearly planar macrocycle core. The angles between the porphyrin plane and the plane of the meso-aryl groups were found to be 81.6 and 83.1°, respectively. As the crystal data (space group, cell dimensions, and angles) as well as bond lengths and angles for

TABLE 1: Selected Bond Lengths and Angles

bond	length (Å)	valence angle	value (deg)
C07−C08	1.416(8)	C08−C07−C09	123.6(5)
C07−C09	1.409(8)	C07−C08−N03	122.4(5)
C09−C11	1.454(8)	C07−C09−N01	122.5(5)
C08−C10	1.473(8)	C08−N03−C14	107.8(4)
C11−C13	1.369(8)	C09−N01−C15	107.7(5)
C10−C12	1.372(8)	N01−C09−C11	109.0(5)
N01−C09	1.375(7)	N03−C08−C10	108.8(4)
N01−C15	1.366(7)	N01−C15−C13	109.4(4)
N03−C08	1.368(7)	N03−C14−C12	109.8(4)
N03−C14	1.367(7)	C08−C10−C12	106.3(5)
C12−C14	1.448(8)	C09−C11−C13	106.4(5)
C13−C15	1.432(8)	C14−C16−C18	131.8(5)
C14−C16	1.391(8)	C06−C07−C08	118.2(5)
C16−C18	1.397(8)	C06−C07−C09	118.1(5)
C06−C07	1.503(7)	C02−C01−C03	122.3(5)

H$_2$DAOAP are in good agreement with those for other published 5,15-diphenyloctaalkyl porphyrins, we chose only to present a few, selected structural parameters in Table 1.[4,10] However, important differences are observed between the meso-diaryl-substituted octaalkyl porphyrins and their structural parents—H$_2$OEP[56] and H$_2$TPP.[57,58] The introduction of two meso-aryl groups has caused a rectangular deformation of the porphyrin core. The N−N separation was found to be 3.183 and 2.695 Å along the meso-phenyl and meso-H axes, respectively, instead of the nearly equal N−N separation in H$_2$OEP and H$_2$TPP. As it has been suggested,[10] it seems reasonable to expect that sterical interactions between the meso-aryls and the neighboring β-alkyl groups cause the in-plane deformation of the porphyrin core along the 5,15-axis. Thus, in the electronic ground state among the two alternative in-plane and out-of-plane macrocycle distortions, the former is still expected to be energetically favorable in 5,15-diaryloctaalkyl porphyrins.

Ground State Absorption and Fluorescence Spectra. The ground state absorption and fluorescence spectra of H$_2$P−RB and ZnP−RB are found to be very similar to the reference compounds H$_2$OEP and ZnOEP, respectively, in terms of band maxima and the full width at half-maximum (fwhm) parameters. These parameters, which are suggested to be sensitive to the conformational flexibility of the macrocycle, do not show significant dependence on solvent polarity and viscosity. Blue shifts of 50−70 cm^{-1} were observed in both the absorption and the emission spectra upon incorporating these porphyrins into a PS film. At 80 K, below the solvent glass-setting temperature, the spectra are practically identical to each other in all of the solvents studied. The fluorescence Stokes shifts for ZnP−BB and ZnP−NB are equal to 150−250 cm^{-1}.

Transient Absorption. The detailed examination of the triplet state decay kinetics of 5,15-diaryloctaalkylporphyrins in MTHF is described in ref 35. Briefly, the transient decays from $T_1 \rightarrow T_n$ absorption are clearly biexponential in the temperature interval 298−175 K, signaling the presence of two triplet
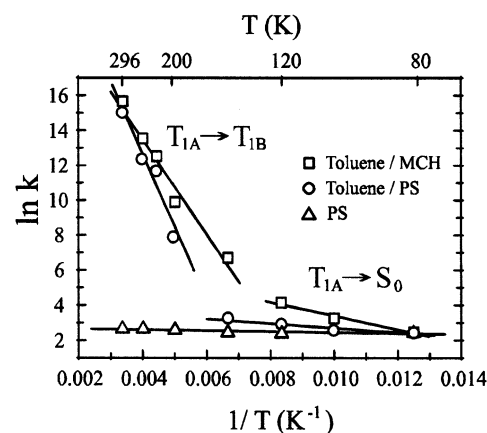

Figure 3. Arrhenius plots of the temperature dependence of the conformational relaxation process $T_{1A} \rightarrow T_{1B}$ and the nonradiative decay $T_{1A} \rightarrow S_0$ for ZnP−BB in toluene/MCH (□), toluene/PS (○) solutions, and PS film (△).

species, arbitrarily called T_{1A} and T_{1B}. The room temperature lifetimes of the two species for ZnP−BB were found to be 86 ns and 5.1 μs, respectively. Also, the 86 ns lifetime was reflected as a rise time in the early part of the transients in the wavelength region where the T_{1B} species is the stronger light absorber. Therefore, we established that there is a mother−daughter relation between the two states, i.e., the T_{1B} species is populated from the T_{1A} species. The 5.1 μs lifetime reflects the subsequent intersystem crossing (isc) process $T_{1B} \rightarrow S_0$. The transformation process $T_{1A} \rightarrow T_{1B}$ is at room temperature estimated to be 6 orders of magnitude more efficient than direct isc $T_{1A} \rightarrow S_0$. Therefore, the T_{1A} state is exclusively deactivated by a transformation process to T_{1B} at room temperature. However, because of the pronounced temperature dependence of the transformation process ($E_a = 6.7$ kcal/mol) and the relative insensitivity of the isc process $T_{1A} \rightarrow S_0$ toward temperature changes ($E_a \leq 0.5$ kcal/mol), the transformation process is virtually shut off at temperatures below 120 K, and the deactivation of the T_{1A} species occurs exclusively by isc to the ground state. The temperature dependence of the decay kinetics in MTHF is similar to what is observed in the solvent mixture toluene/MCH (see Table 2 and Figure 3). It has been suggested that the cis tautomer of free base porphyrins has lower energy than the trans tautomer in the triplet state.[59] Therefore, a tautomerization reaction could in principle be responsible for the conversion of T_{1A} into T_{1B}; however, this is unlikely since we observe the same processes for both free base and zinc porphyrins. The large viscosity dependence (vide infra) and activation energy for the reaction also go against a proton tunneling process in the core of the porphyrin as the process responsible for the observed triplet state dynamics. To investigate the nature of the transformation process, we have studied these compounds in an extended series of solvent mixtures with different viscosities.

TABLE 2: Triplet Lifetime of Zn−RB Derivatives in Various Solvents at Different Temperatures

	ZnP−BB					ZnP−NB				
	toluene/MCH		toluene/PS		PS	toluene/MCH		toluene/PS		PS
T (K)	τ_A (μs)	τ_B (μs)	τ_A (μs)	τ_B (μs)	τ (μs)	τ_A (μs)	τ_B (μs)	τ_A (μs)	τ_B (μs)	τ (μs)
295	0.17	6.0	0.29	9.0	66 000	0.15	5.7	0.31	9.2	65 000
250	1.5	7.9	4.2	12.3	76 000	1.4	7.6	4.1	13.0	76 000
225	3.7	15	6.5	36		3.5	14	6.4	34	
200	53		380		80 000	48		400		81 000
150	1300		43 000		82 000	1300		42 000		83 000
120	16 000		54 000		85 000	16 000		56 000		86 000
100	40 000		73 000			37 000		75 000		
80	84 000		90 000		90 000	84 000		90 000		91 000

Porphyrins in the Excited Triplet State

J. Phys. Chem. B, Vol. 106, No. 48, 2002 **12617**

TABLE 3: Triplet Lifetime of Free Base Porphyrin Derivatives in Various Solvents at Different Temperatures

	H₂P−BB						H₂P−NB					
	toluene/MCH		MTHF		toluene/PS		toluene/MCH		MTHF		toluene/PS	
T (K)	τ_A (μs)	τ_B (μs)	τ_A (μs)	τ_B (μs)	τ_A (μs)	τ_B (μs)	τ_A (μs)	τ_B (μs)	τ_A (μs)	τ_B (μs)	τ_A (μs)	τ_B (μs)
295	0.13	9.1	0.14	8.9	0.32	17.3	0.15	9.4	0.14	8.0	0.30	15.6
250	1.17	13.1	1.09	13.6	3.46	23.6	1.21	13.2	1.31	12.2	3.72	22.1
225	3.82	29.5			7.36	65.0	3.95	31.2			7.55	64.0
200	105		191	38.0	540		120		177	66.4	550	
150	1390				9900		1500				10100	
120	5700				13000		5600				12000	
100	7700				14500		7900				14000	
80	9400				15000		9600				15500	

TABLE 4: Preexponential Factors (A) and Activation Energies (E_a) of the Excited Triplet State $T_{1A} \rightarrow T_{1B}$ Relaxation Process in Different Solvents

	ZnP−BB		H₂P−BB		ZnP−NB		H₂P−NB	
solvent	A (s^{-1})	E_a (kcal/mol)	A (s^{-1})	E_a (kcal/mol)	A (s^{-1})	E_a (kcal/mol)	A (s^{-1})	E_a (kcal/mol)
toluene/MCH (1:6)	3.9×10^{10}	5.4	3.3×10^{11}	6.3	4.9×10^{10}	5.5	2.1×10^{11}	6.1
2-MTHF^a	1.1×10^{12}	6.7	1.4×10^{12}	7.1	1.0×10^{12}	6.6	5.0×10^{12}	7.8
toluene/PS (1:1)	5.5×10^{12}	8.3	11.0×10^{12}	8.7	5.3×10^{12}	8.1	13.0×10^{12}	8.8

^{a} Ref 35.

Viscosity Dependence. The solvents/solvent mixtures used in the study are, in order of increasing viscosity, toluene/MCH, toluene/PS, and PS film. As we believe that the transformation process involves conformational changes of the porphyrin macrocycle, the rate of the process should be sensitive toward solvent viscosity. The resulting lifetimes from the transient absorption measurements are presented in Tables 2 and 3. Assuming the rate constants (and the corresponding lifetimes) to follow an Arrhenius type of expression

$$k = A \cdot \exp(-E_a/RT) \tag{1}$$

$\ln(1/\tau)$ plotted vs $1/T$ yields the preexponential factor A and the activation energy E_a through the intersection and the slope, respectively. Figure 3 shows the Arrhenius plot for ZnP−BB in the different solvents, and the Arrhenius parameters are collected in Table 4. It is immediately obvious that the behavior in the PS matrix is dramatically different from the low viscous solvents; in particular, the absence of a short lifetime in PS could be noted. The measurements suggest that in PS, the DAOAP derivatives are deactivated by one single, virtually temperature-independent process over the entire temperature interval 295−80 K. As the rate constant of this process corresponds well to the isc process $T_{1A} \rightarrow S_0$ observed in the other solvents, it is obvious that no transformation $T_{1A} \rightarrow T_{1B}$ occurs in the highly viscous PS film. In the solvent mixtures toluene/MCH and toluene/PS, the decays are clearly biexponential at higher temperatures, which indicates that the transformation process is operative in both solvent mixtures. However, the temperature effect on the rate of the transformation process depends strongly on the solvent viscosity. As seen in Figure 3 and Table 4, the response on lowering the temperature is much more pronounced in the more viscous solvent mixture (E_a = 5.4 and 8.3 kcal/mol for toluene/MCH and toluene/PS, respectively). This indicates that in addition to the intrinsic activation energy, there is a substantial contribution from a viscosity associated "friction". A similar behavior is observed for the other DAOAP derivatives (see Table 4). Thus, the results from transient absorption measurements support the notion that conformational changes are involved in the transformation process.

DFT Calculations. *S_0 and T_1 Geometries of H₂OMP.* The optimized geometry of H₂OMP in the electronic ground state was obtained at the RB3LYP/6-31G(d) level. The unconstrained

optimization converged to a stable structure of D_{2h} symmetry. The same minimal energy geometry was found whether the optimization was symmetry-constrained or not. The most important ground state structural parameters of the porphyrin skeleton are presented in Figure 4 (bottom values in italic). The calculated bond lengths of the porphyrin core were found in close agreement with X-ray data for the structurally similar H₂-OEP[56] and are also very similar to the values obtained for H₂P[38−41] at different DFT levels.

The fully optimized geometry of H₂OMP in the T_1 state was obtained with a spin-unrestricted wave function at the same DFT level (Figure 4, top values). However, upon the UB3LYP/6-31G(d) optimization, the initial structure, corresponding to the S_0 symmetry, was found unstable with regard to relaxation toward a structure of lower symmetry. The T_1 optimization of H₂OMP converged to a structure of C_{2v} symmetry. The most noticeable structural changes observed in H₂OMP upon the $S_0 \rightarrow T_1$ excitation are characterized by bond length alternation around the porphyrin macrocycle. The main structural changes
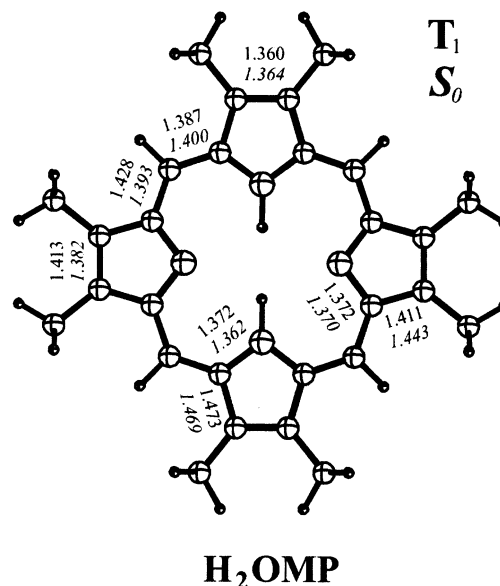
Figure 4. Geometry and selected bond lengths (in Ångström) for H₂-OMP in the S_0 (bottom, italic) and T_1 (top, normal) states obtained at the B3LYP/6-31G(d) level.
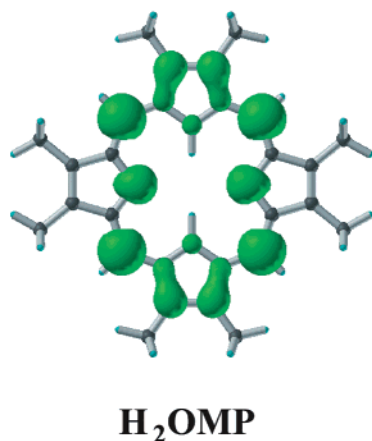
H₂OMP

Figure 5. Unpaired spin density isosurface (0.003 e/au³) computed for H₂OMP at the UB3LYP/6-31G(d) level.

are localized in the pair of opposite pyrrole units that carries N-hydrogens, whereas the geometry of the other pair is found almost unchanged. As a result of the structural changes accompanying the $S_0 \rightarrow T_1$ excitation, the inner core size of the porphyrin skeleton, determined by the four pyrrole nitrogen atoms, expanded, so that the N—N distances between the opposite pyrrole units were found to be 4.088 and 4.282 Å in the T_1 state as compared to 4.066 and 4.230 Å in S_0. Please note that the nitrogens in H₂OMP are at the corners of a rhombus and that the N—N distances along the two axes defined by the meso carbons are almost identical.

Recent studies by Nguyen and co-workers[42−45] have reported the UB3LYP/6-31G(d) triplet state structure of H₂P. The same general trends in the structural changes accompanying the $S_0 \rightarrow T_1$ excitation were observed. The bond length alternation was also found to lie within 0.03 Å. Thus, comparison of these results with our results for H₂OMP has shown that the porphyrin skeleton planarity is not significantly perturbed by the introduction of the peripheral β-methyl groups.

Electronic Structure and Spin Density Distribution for H₂OMP in the T_1 State. The low-lying excited singlet and triplet states of porphyrins can be described according to the Gouterman four orbital model.[60] Within this model, the S_1 and T_1 states of porphyrins can be modeled in terms of electronic transitions between each of the two highest occupied molecular orbitals (HOMOs), a_{1u} (π) and a_{2u} (π), to the two degenerate or pseudo-degenerate LUMOs, e^*_g (π) (all orbitals are labeled according to D_{4h} symmetry). There is a strong mixing between the $^1(a_{1u}e_g)$ and $^1(a_{2u}e_g)$ electronic configurations for the lowest excited singlet state. However, the lowest excited triplet state can be described[61−63] by a single electron HOMO−LUMO excitation. The lowest triplet state of H₂OMP was found to be the $^3B_1$ state. Thus, in H₂OMP, the $S_0 \rightarrow T_1$ excitation removes one electron from the HOMO and adds one electron to the LUMO; thereby, this process should change the electron density distribution, which then is followed by bond length changes. Adding or removing one electron can be potentially responsible for bond length shortening or elongating, depending on which of the bonding or antibonding orbital nodal patterns are involved in the electronic transition.

Figure 5 shows the Mulliken spin density distribution that represents the delocalization of an unpaired α-electron in H₂-OMP. The unpaired spin density profile matches the shape of the LUMO of H₂OMP. A distinctive feature of the distribution is the high atomic spin density localization at the meso carbons. The opposite meso carbons of the macrocycle bear an α-spin density equal to 0.37−0.39 electrons. There is also a significant
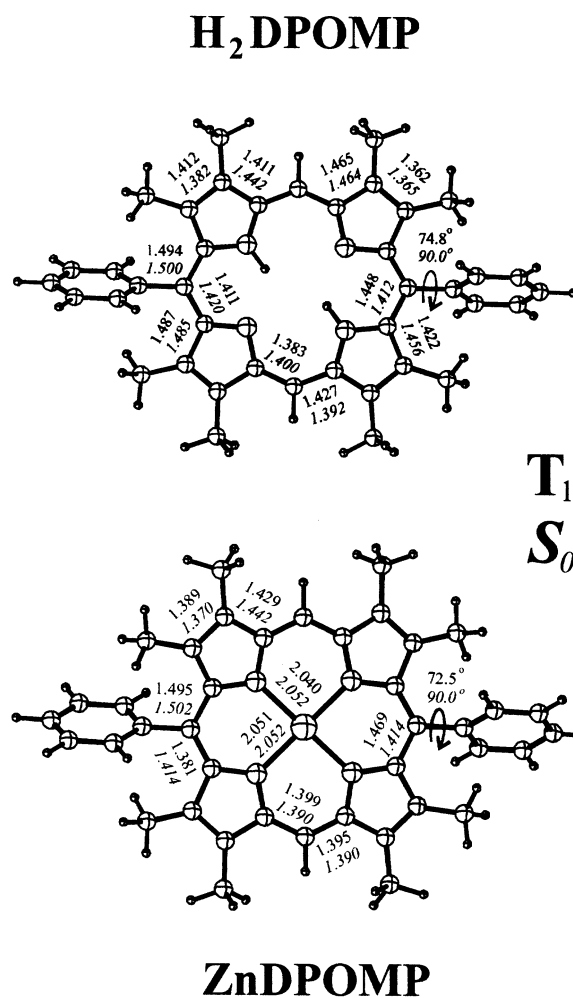
H₂DPOMP

T_1

S_0

ZnDPOMP

Figure 6. Geometries and selected bond lengths (in Ångström) and angles (in degrees) for H₂DPOMP and ZnDPOMP in the S_0 (bottom, italic) and T_1 (top, normal) states obtained at the B3LYP/6-31G(d) level.

density on one of the pair of the opposite pyrrole units (Figure 5). Thus, the asymmetry of the observed structural rearrangement can be explained by the nature of the $S_0 \rightarrow T_1$ excitation localization in which the main contribution is expected to be due to the HOMO−LUMO transition.

S_0 and T_1 Geometries of H₂DPOMP and ZnDPOMP. The ground state RB3LYP/6-31G(d) optimization converged to a minimum energy structure of C_{2h} and D_{2h} symmetry for H₂-DPOMP and ZnDPOMP, respectively. Thus, both of the structures are characterized by a flat porphyrin macrocycle and orthogonal meso-phenyl planes. For H₂DPOMP, the bond length parameters agree well with the X-ray data for H₂DAOAP (cf. Figures 2 and 6, Table. 1). As compared to OMP, the main structural changes, caused by the phenyl substituents, consist of a deformation of the porphyrin macrocycle from the typical square geometry to a rectangular elongated structure (Figure 6). The N—N distance along the *x*- and *y*-axes is calculated to be 3.230 and 2.706 Å in H₂DPOMP as compared to the X-ray values of 3.183 and 2.695 Å. In ZnDPOMP, the rectangular deformation is smaller and these values are equal to 2.981 and 2.820 Å. Both X-ray data and the DFT calculations demonstrate that due to the introduction of bulky peripheral phenyl groups, both H₂DPOMP and ZnDPOMP experience considerable sterical forces, which cause the in-plane deformation of the macrocycle along the meso phenyl axis.

One of the most intriguing findings of this study was that the reoptimization of the ground state geometry of H₂DPOMP
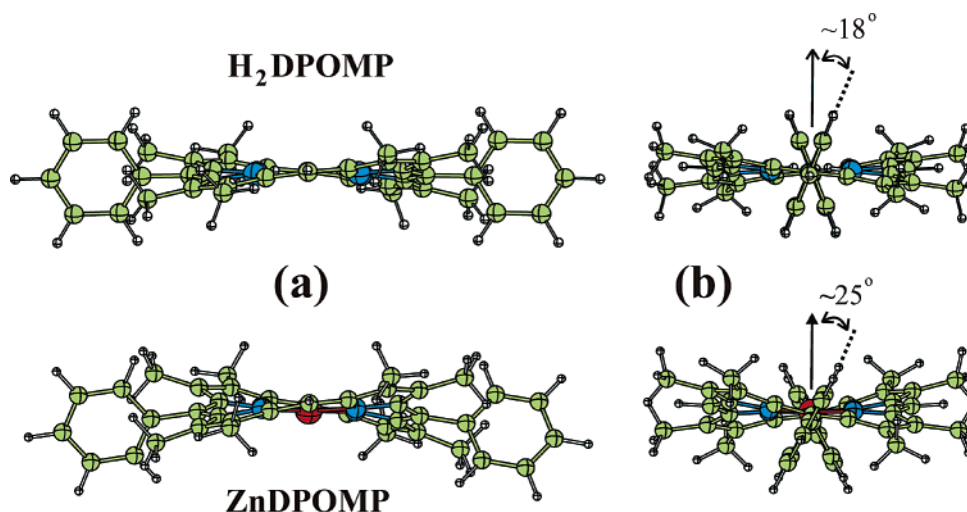
Porphyrins in the Excited Triplet State

J. Phys. Chem. B, Vol. 106, No. 48, 2002 **12619**

Figure 7. Two views along the short (a) and long (a) molecular axis for the saddle-shaped T_1 state conformation of H_2DPOMP and ZnDPOMP.

and ZnDPOMP at the UB3LYP/6-31G(d) level converged to the strongly nonplanar porphyrin conformation in the lowest triplet state (Figures 6 and 7). The relaxed geometry, consisting of the up and down out-of-plane deviations of the pyrrole rings, corresponds to a saddle-shaped conformation (Figure 7). The magnitude of macrocycle saddling is different for H_2DPOMP and ZnDPOMP, but the mode of distortion is very similar.[64] We have carried out an extensive search on the conformational space by starting the optimization from different initial geometries, including those of the mentioned S_0 planar geometry, several saddle-shaped conformations with various degrees of saddling, and a few ruffle-shaped geometries. In all cases, the optimizations converged to the same nonplanar saddle conformation. The saddle conformation of H_2DPOMP was found to have C_2 symmetry. The lowest energy conformation of ZnDPOMP was found to have only C_1 symmetry.

The bond alternant structure, observed for H_2OMP in the T_1 state, is also found for the conformationally distorted skeleton of the meso-diphenyl derivatives. The bond lengths of one pair of the opposite pyrrole rings are strongly alternant, while those of the other pair are almost equal, similar to the unsubstituted OMP.

Despite the strong nonplanar deformation of the porphyrin macrocycle in ZnDPOMP, the four inner N atoms and the central Zn ion still form a plane with an average out-of-plane deviation of 0.15 Å. It is interesting to note that the size of the central rectangular core, defined by these four pyrrole nitrogens, is almost unchanged. As it can be seen from Figures 6 and 7, the meso-phenyl units of ZnDPOMP in the T_1 state are no longer orthogonal to the porphyrin plane. The meso-phenyl groups in H_2DPOMP and ZnDPOMP adopt dihedral angles of 74.8 and 72.5° toward the porphyrin plane. Such a rotation might potentially account for a more efficient orbital overlap and better π-electronic conjugation to the adjacent chromophore in D−B−A systems.

We could not find stationary points on the T_1 surface, which corresponds to the conformer of H_2DPOMP and ZnDPOMP with a planar porphyrin macrocycle (model for the observed T_{1A} state). Several starting points for the optimization were tested and showed that the triplet state surface around the planar minimum is very flat and that the barrier separating the planar from the saddled conformer is very small. Experimentally, it seems reasonable to assume that the initially populated triplet state is planar since the T_{1A} state is spectrocopically similar to other porphyrins with normal photophysics. A planar conformer
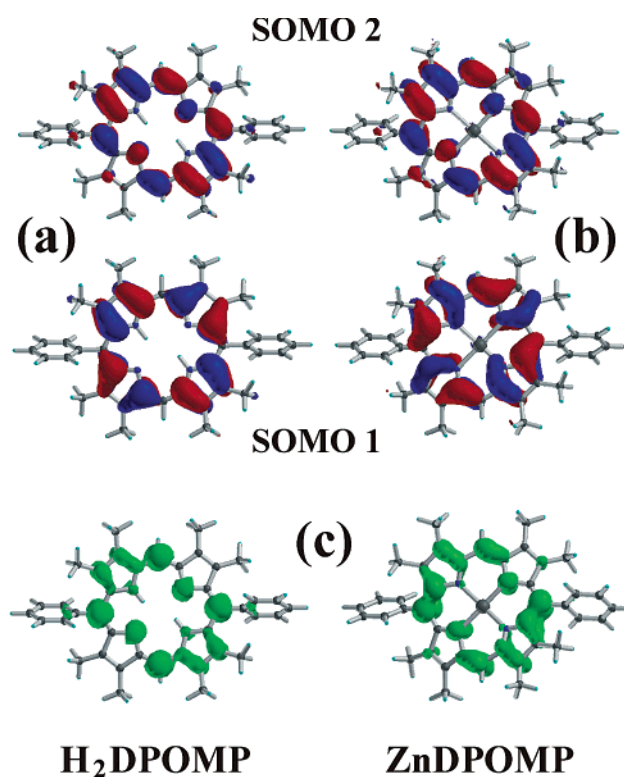

Figure 8. Relaxed singly occupied molecular orbitals (SOMO) of H_2-DPOMP (a) and ZnDPOMP (b) calculated at the UB3LYP/6-31G(d) level. All orbitals are contoured at 0.025 e/au³. Panel c shows unpaired spin density isosurfaces (0.003 e/au³) computed at the same level.

with orthogonally constrained phenyl rings was therefore used to mimic the structural changes occurring in the rest of the molecule of the initially populated T_{1A} conformer. The partially relaxed conformer has a bond alternant structure, which is very similar in many respects to the fully relaxed geometry of the corresponding reference compounds.

Electronic Structure and Spin Density Distribution of H_2DPOMP and ZnDPOMP in the T_1 State. The two relaxed single occupied molecular orbitals (SOMO) of the saddle-shaped conformations of H_2DPOMP and ZnDPOMP are shown in Figure 8a,b. The shape of the frontier orbitals of H_2DPOMP is found to be similar to that of the corresponding S_0 orbitals, whereas in the case of ZnDPOMP, the SOMOs revealed a more complicated shape, which can be explained by the more pronounced macrocycle distortions. The lowest triplet state for
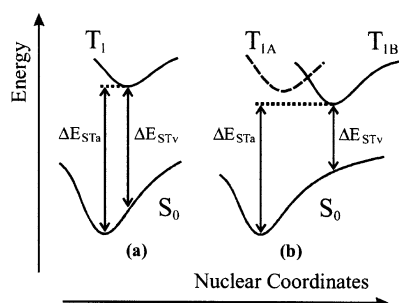
Figure 9. Schematic diagram for the S_0 and the T_1 state surfaces with one (a) or two (b) excited state energy minima. See text for details.

H_2DPOMP and $ZnDPOMP$ is the ^3B state. Thus, the $S_0 \rightarrow T_1$ excitation involves the same set and order of frontier orbitals in both porphyrins; hence, the T_1 state is expected to have the same electronic origin as for the corresponding H_2OMP compound.

The spin density distribution for the T_1 saddle-shaped conformation of H_2DPOMP and $ZnDPOMP$ is shown in Figure 8c. Similarly to the reference compound, the spin density profile matches the shape of the LUMO. High atomic spin densities were found on the meso carbons and on one pair of the pyrrole rings. Because of the saddle distortions, the spin distribution becomes more delocalized through the macrocycle as compared to the planar reference porphyrins.

J−T Effects in the T_1 State. Within the framework of a single electron excitation, the degenerate e^*_g LUMOs of metalloporphyrins of D_{4h} symmetry become partially occupied in the T_1 state. According to the J−T theorem,[65] such a triplet with doubly degenerate electronic states is expected to be unstable at the highly symmetric configurations and is allowed to relax toward a new stationary point of lower symmetry. Most of the available experimental resonance Raman studies have suggested that these kinds of J−T distortions are operative in metalloporphyrins in the lowest triplet state[66] and also in the π-monoanion radical.[67]

The J−T theorem can be strictly applied for porphyrins with D_{4h} symmetry. The formal symmetry of H_2DPOMP and $ZnDPOMP$ in the ground state is C_{2h} and D_{2h}, respectively. However, it is reasonable to expect the higher effective symmetry of the porphyrin chromophore in these molecules. The orthogonal meso-phenyl groups do not extend significantly the overall molecular π-system. Thus, the frontier orbitals undergo a relatively small perturbation and their symmetry is close to that of the reference porphyrins. The two LUMOs of H_2DPOMP and $ZnDPOMP$ are not completely degenerated, but their energy splitting is found to be relatively small, 0.02 and 0.03 eV, respectively.

It has been shown that ZnTPP in the T_1 state undergoes J−T deformations.[22,23,30] It has also been demonstrated[68] that the meso-diphenyl-substituted zinc porphyrin of the D_{2h} formal symmetry revealed temperature-dependent changes in the EPR spectra, which could be explained in terms of dynamic J−T distortions, suggesting the effective D_{4h} symmetry of the porphyrin chromophore. On this basis, we expect that the pseudo-J−T distortions might still be operative in the initially populated planar T_{1A} state in both H_2DPOMP and $ZnDPOMP$. The dynamic in-plane distortions along the J−T active vibrational modes are able to initiate the out-of-plane conformational relaxation process that is further driven to the T_{1B} state by the tendency to minimize the sterical strain energy.

S_0 and T_1 Potential Energy Surfaces. The shape of the S_0 and T_1 surfaces was reconstructed on the basis of their adiabatic

TABLE 5: Adiabatic ΔE_{STa} and Vertical Relaxed ΔE_{STv} Energy Gaps (in eV) calculated at the B3LYP/6-31G(d) Level

compds	adiabatic (S_0−T_1)			vertical($T_1 \rightarrow S_0$)		experiment[e]
	ΔE_{STa}		ΔH_{ST}	ΔE_{STv}		
H_2OMP	1.59		1.47	1.35		1.61[a,b,d]
	T_{1A}	T_{1B}		T_{1A}	T_{1B}	
H_2DPOMP	1.65	1.56	1.45	1.51	1.29	1.54[a,b]
$ZnDPOMP$	1.87	1.74		1.72	1.43	1.73[c]

[a] Ref 33. [b] Ref 34. [c] Ref 35. [d] Ref 68. [e] 0−0 transitions estimated from onset of the phosphorescence spectra.

and vertical energy differences calculated for a few selected points. Two approaches were considered. The first one was based on the R- and UB3LYP energies for the optimized S_0 and T_1 structures. Alternatively, the vertical S_0−T_1 energy difference was obtained for the same geometries by the TD-DFT method. At first, the analysis was done for the H_2OMP reference compound. These results are compared with the available experimental phosphorescence data for structurally similar porphyrins to estimate the reliability of both approaches. The calculations were repeated for H_2DPOMP and $ZnDPOMP$. The main goal of this part of the work is to examine how the $T_{1A} \rightarrow T_{1B}$ conformational relaxation in the diaryloctaalkyl porphyrins influences the S_0−T_1 energy gap.

The adiabatic S_0−T_1 energy gap ΔE_{STa} for H_2OMP (Figure 9) was calculated as the difference between the R- and UB3LYP/6-31G(d) energies of the fully optimized S_0 and T_1 structures. The zero-point energy correction for ΔE_{STa} was also included, and these results are presented as ΔH_{ST} in Table 5. The vertical S_0−T_1 energy gap ΔE_{STv} was obtained as the difference between the energy of the relaxed T_1 state and the ground state energy corresponding to this T_1 geometry. The later value of ΔE_{STv} can be directly compared with the experimental determined phosphorescence energy. For H_2OMP, both the vertical and the adiabatic S_0−T_1 energy splitting are found to be in fair agreement with the phosphorescence data for H_2OEP reported by Zenkevich[33,34] and also by Leung.[69]

The conformational relaxation of the diaryloctaalkyl porphyrins in the T_1 state is believed to involve the two state model.[35] Therefore, we consider the saddle-shaped minimal energy conformation of H_2DPOMP and $ZnDPOMP$ as the final T_{1B} state of the relaxation process. The initially populated T_{1A} state was modeled by the partially optimized structure in which the porphyrin skeleton was allowed to relax during the optimization, but the meso-phenyl groups were orthogonally constrained. In this way, the planarity of the porphyrin macrocycle of the T_{1A} conformation was restrained. The energy of this structure was used for the calculation of the T_{1A} state energetics. The adiabatic and vertical energy gap values for both the T_{1A} and the T_{1B} states of H_2DPOMP and $ZnDPOMP$ were calculated by the same procedure as in the case of the reference porphyrins (Table 5). The zero-point energy corrected value, ΔH_{ST}, for the T_{1B} state was also calculated.

The calculated adiabatic ΔE_{STa} energy difference between the T_{1A} and the T_{1B} states was found to be quite small, within 0.09− 0.13 eV for H_2DPOMP and $ZnDPOMP$. Thus, the T_{1A} structure was found only 2.1 and 3.0 kcal/mol less stable than the fully relaxed T_{1B} conformer of H_2DPOMP and $ZnDPOMP$, respectively. However, the experimentally observed phosphorescence is expected to originate from the initially populated T_{1A} state because the $T_{1A} \rightarrow T_{1B}$ conformational relaxation is hindered at low temperature. Both calculated ΔE_{STa} energies agree with the experimental values. The vertical energy gap for the saddle-shaped conformer was found significantly decreased by 0.27

Porphyrins in the Excited Triplet State

J. Phys. Chem. B, Vol. 106, No. 48, 2002 **12621**

TABLE 6: Three Lowest Vertical $S_0 \rightarrow T_{1A}$ and $S_0 \rightarrow T_{1B}$ Excitation Energies (in eV) for the Reference and Model Porphyrins Calculated at the TD-RB3LYP/6-31G(d) Level

vertical excitation to the T_{1A} state[a] $S_0(T_{1A}) \rightarrow T_{1A}$		vertical excitation to the T_{1B} state[b] $S_0(T_{1B}) \rightarrow T_{1B}$	
electronic states	$\Delta E_{ST}(T_{1A})$	electronic states	$\Delta E_{ST}(T_{1B})$
H₂OMP			
$1\,^3B_{2u}$	1.49	$1\,^3B_1$	1.12
$2\,^3B_{3u}$	1.85	$2\,^3B_2$	1.80
$3\,^3B_{2u}$	1.95	$3\,^3B_2$	1.98
H₂DPOMP			
$1\,^3B_u$	1.48	$1\,^3B$	1.07
$2\,^3B_u$	1.82	$2\,^3B$	1.78
$3\,^3B_u$	1.94	$3\,^3B$	1.89
ZnDPOMP			
$1\,^3B_{3u}$	1.74	$1\,^3B$	1.33
$2\,^3B_{2u}$	1.76	$2\,^3B$	1.68
$3\,^3B_{2u}$	2.03	$3\,^3B$	1.92

[a] Calculated at the optimized ground state geometry. [b] Calculated at the relaxed triplet state geometry.

and 0.31 eV from those of the adiabatic case. The energy rising of the S_0 surface upon the saddle-shaped distortion of the porphyrin macrocycle is apparently responsible for the observed pronounced decrease in energy slitting between the T_1 and the S_0 state surfaces. These results give some evidence that the potential energy surface of the T_1 state is less sensitive to the out-of-plane distortions of a porphyrin macrocycle than the S_0 one, and this also means that the T_1 surface is relatively flat. The vertical $S_0 \rightarrow T_1$ excitation energy was also calculated and found to be 1.85 eV. Thus, the $S_0 - T_1$ energy gap dependence upon the $T_{1A} \rightarrow T_{1B}$ conformational relaxation for H₂DPOMP can be reconstructed as follows: The direct vertical $S_0 \rightarrow T_1$ excitation of 1.85 eV is followed by bond length readjustments within the planar porphyrin macrocycle, and these structural changes stabilize the energy of the T_{1A} state to 1.65 eV. In the next step, the T_{1A} structure undergoes a saddle-shaped distortion to the T_{1B} conformer, which is further stabilized to 1.56 eV above the optimized S_0 state minimum.

The ΔE_{ST} values were also alternatively calculated at the TD-DFT B3LYP-6-31G(d) level. The ΔE_{ST} ($S_0 \rightarrow T_1$) vertical excitation energy was determined for the S_0 optimized geometry, whereas the vertical ΔE_{ST} ($T_1 \rightarrow S_0$) energy gap was obtained for the relaxed T_1 state structure. In the case of the H₂OMP model compound, the ΔE_{ST} value was found in agreement with the experimentally determined $S_0 - T_1$ energy splitting (Tables 5 and 6). These values are also close to the corresponding adiabatic ΔE_{ST} splitting. However, the ΔE_{ST} ($T_1 \rightarrow S_0$) gap for the saddle-shaped H₂DPOMP and ZnDPOMP was found significantly decreased by 0.31 and 0.41 eV relative to the value of the ΔE_{ST} ($S_0 \rightarrow T_1$) vertical excitation (Table 6). Thus, similarly to the previous approach based on the adiabatic ΔE_{STa} and the ground state energy corrected, vertical ΔE_{STv} values, these TD-DFT results also predict a significant decrease of the $S_0 - T_1$ energy splitting upon conformational relaxation in the excited triplet state.

Conclusions

There is a significant temperature and viscosity dependence on the triplet dynamics of *meso*-diphenyloctaalkylporphyrins. A series of experiments show that this class of porphyrins undergoes a conformational transformation on the triplet surface and that this leads to a substantial shortening of the triplet lifetime. With the aid of DFT calculations, an out-of-plane distorted conformer on the triplet surface was identified and

structurally characterized. The most stable triplet structure adopted a saddle-shaped conformation as a result of balancing sterical forces and electronic factors. It is conceivable that the increased nonradiative decay is related to this structural deformation since the energy gap between the lowest triplet and the ground states is significantly reduced. In addition, we have observed that triplet energy transfer in donor−acceptor molecules employing these porphyrins (Chart 2) is dramatically reduced in high viscous media.[55] By structural relaxation of the donor, the electronic coupling to the acceptor is substantially increased. Because both the triplet energy transfer process and the structural relaxation occur on the same time scale, there is a mutual dynamic coupling. This phenomenon might be used to gate the transfer process, and it will be investigated soon along with an attempt to experimentally identify and characterize the transient triplet species by either time-resolved IR or Raman spectroscopy.

Supporting Information Available: A listing of all S_0 and T_1 optimized geometries (Cartesian coordinates). This material is available free of charge via the Internet at http://pubs.acs.org.

References and Notes

(1) Shelnutt, J. A.; Song, X.-Z.; Ma, J.-G.; Jia, S.-L.; Jentzen, W.; Medforth, C. J. *Chem. Soc. Rev.* **1998**, *27*, 31.
(2) Ravikanth, M.; Chandrashekar, T. K. *Struct. Bonding* **1995**, *82*, 105.
(3) Jentzen, W.; Ma, J.-G.; Shelnutt, J. A. *Biophys. J.* **1998**, *74*, 753.
(4) Senge, M. O.; Kalisch, W. W. *Inorg. Chem.* **1997**, *36*, 6103.
(5) Sazanovich, I. V.; Galievsky, V. A.; van Hoek, A.; Schaafsma, T. J.; Malinovskii, V. L.; Holten, D.; Chirvony, V. S. *J. Phys. Chem. B* **2001**, *105*, 7818.
(6) Senge, O. M.; Renner, M. W.; Kalisch, W. W.; Fajer, J. *J. Chem. Soc.*, Dalton Trans. **2000**, 381.
(7) Muzzi, C. M.; Medforth, C. J.; Smith, K. M.; Jia, S.-L.; Shelnutt, J. A. *Chem. Commun.* **2000**, 131.
(8) Gentemann, S.; Nelson, N. Y.; Jaquinod, L.; Nurco, D. J.; Leung, S. H.; Medforth, C. J.; Smith, K. M.; Fajer, J.; Holten, D. *J. Phys. Chem. B* **1997**, *101*, 1247.
(9) Gentemann, S.; Medforth, C. J.; Forsyth, T. P.; Nurco, D. J.; Smith, K. M.; Fajer, J.; Holten, D. *J. Am. Chem. Soc.* **1994**, *116*, 7363−7368.
(10) Senge, M. O.; Medforth, C. J.; Forsyth, T. P.; Lee, D. A.; Olmstead, M. M.; Jentzen, W.; Pandey, R. K.; Shelnutt, J. A.; Smith, K. M. *Inorg. Chem.* **1997**, *36*, 1149.
(11) Barkigia, K. M.; Berber, M. D.; Fajer, J.; Merforth, C. J.; Renner, M. W.; Smith, K. M. *J. Am. Chem. Soc.* **1990**, *112*, 8851.
(12) Hobbs, J. D.; Majumder, S. A.; Luo, L.; Sickelsmith, G. A.; Quirke, J. M. E.; Medforth, C. J.; Smith, K. M.; Shelnutt, J. A. *J. Am. Chem. Soc.* **1994**, *116*, 3261.
(13) Cupane, A.; Leone, M.; Unger, E.; Lemke, C.; Beck, M.; Dreybrodt, W.; Schweitzer-Stenner, R. *J. Phys. Chem. B* **1998**, *102*, 6612.
(14) Sparks, L. D.; Medforth, C. J.; Park, M.-S.; Chamberlain, J. R.; Ondrias, M. R.; Senge, M. O.; Smith, K. M.; Shelnutt, J. A. *J. Am. Chem. Soc.* **1993**, *115*, 581.
(15) Anderson, K. K.; Hobbs, J. D.; Luo, L.; Stanley, K. D.; Quirke, J. M. E.; Shelnutt, J. A. *J. Am. Chem. Soc.* **1993**, *115*, 12346.
(16) Retsek, J. L.; Medforth, C. J.; Nurco, D. J.; Getemann, S.; Chirvony, V. S.; Smith, K. M.; Holten, D. *J. Phys. Chem. B* **2001**, *105*, 6396.
(17) Retsek, J. L.; Getemann, S.; Medforth, C. J.; Smith, K. M.; Chirvony, V. S.; Fajer, J.; Holten, D. *J. Phys. Chem. B* **2000**, *104*, 6690.
(18) Chirvony, V. S.; van Hoek, A.; Galievsky, V. A.; Sazanovich, I. V.; Schaafsma, T. J.; Holten, D. *J. Phys. Chem. B* **2000**, *104*, 9909.
(19) Drain, C. M.; Gentemann, S.; Roberts, J. A.; Nelson, N. Y.; Medforth, C. J.; Jia, S.; Simpson, M. C.; Smith, K. M.; Fajer, J.; Shelnutt, J. A.; Holten, D. *J. Am. Chem. Soc.* **1998**, *120*, 3781.
(20) Gudowska-Nowak, E.; Newton, M. D.; Fajer, J. *J. Phys. Chem.* **1990**, *94*, 5795.
(21) Gentemann, S.; Medforth, C. J.; Ema, T.; Nelson, N. Y.; Smith, K. M.; Fajer, J.; Holten, D. *Chem. Phys. Lett.* **1995**, *245*, 441.

Kyrychenko et al.

(22) Walters, V. A.; de Paula, J. C.; Babcock, G. T.; Leroi, G. E. *J. Am. Chem. Soc.* **1989**, *111*, 8300.

(23) Reed, R. A.; Purrello, R.; Prendergast, K.; Spiro, T. G. *J. Phys. Chem.* **1991**, *95*, 9720.

(24) Perng, J.-H.; Bocian, D. F. *J. Phys. Chem.* **1992**, *96*, 4804.

(25) Kumble, R.; Hu, S.; Loppnow, G. R.; Vitols, S. E.; Spiro, T. G. *J. Phys. Chem.* **1993**, *97*, 10521.

(26) Kreszowski, D. H.; Deinum, G.; Babcock, G. T. *J. Am. Chem. Soc.* **1994**, *116*, 7463.

(27) Sato, S.-I.; Asano-Someda, M.; Kitagawa, T. *Chem. Phys. Lett.* **1992**, *189*, 443.

(28) Bell, S. E. J.; Al-Obaidi, A. H. R.; Hegarty, M.; Hester, R. E.; McGarvey, J. J. *J. Phys. Chem.* **1993**, *97*, 11599.

(29) Bell, S. E. J.; Al-Obaidi, A. H. R.; Hegarty, M.; McGarvey, J. J.; Hester, R. E. *J. Phys. Chem.* **1995**, *99*, 3959.

(30) Bell, S. E. J.; Aakeröy, C. B.; Al-Obaidi, A. H. R.; Hegarty, J. N. M.; McGarvey, J. J.; Lefley, C. R.; Moore, J. N.; Hester, R. E. *J. Chem. Soc., Faraday Trans.* **1995**, *91*, 411.

(31) Canters, G. W.; Jansen, G.; Noort, M.; van der Waals, J. H. *J. Phys. Chem.* **1976**, *80*, 2253.

(32) Prendergast, K.; Spiro, T. G. *J. Phys. Chem.* **1991**, *95*, 9728.

(33) Knyukshto, V.; Zenkevich, E.; Sagun, E.; Shulga, A.; Bachilo, S. *Chem. Phys. Lett.* **1998**, *297*, 97.

(34) Knyukshto, V. N.; Sagun, E. I.; Shulga, A. M.; Bachilo, S. M.; Zenkevich, E. I. *J. Fluoresc.* **2000**, *10*, 55.

(35) Andréasson, J.; Zetterqvist, H.; Kajanus, J.; Mårtensson, J.; Albinsson, B. *J. Phys. Chem. A* **2000**, *104*, 9307.

(36) Regev, A.; Galili, T.; Medforth, C. J.; Smith, K. M.; Barkigia, K. M.; Fajer, J.; Levanon, H. *J. Phys. Chem.* **1994**, *98*, 2520.

(37) Michaeli, S.; Soffer, S.; Levanon, H.; Senge, M. O.; Kalisch, W. W. *J. Phys. Chem. A* **1999**, *103*, 1950.

(38) Almlöf, J.; Fischer, T. H.; Gassman, P. G.; Ghosh, A.; Häser, M. *J. Phys. Chem.* **1993**, *97*, 10964.

(39) Ghosh, A. *Acc. Chem. Res.* **1998**, *31*, 189.

(40) Ghosh, A.; Vangberg, T. *Theor. Chem. Acc.* **1997**, *97*, 143.

(41) Nguyen, K. A.; Pachter, R. *J. Chem. Phys.* **2001**, *114*, 10757.

(42) Nguyen, K. A.; Day, P. N.; Pachter, R. *J. Chem. Phys.* **1999**, *110*, 9135.

(43) Nguyen, K. A.; Day, P. N.; Pachter, R. *J. Phys. Chem. A* **1999**, *103*, 9378.

(44) Nguyen, K. A.; Day, P. N.; Pachter, R. *J. Phys. Chem. A* **2000**, *104*, 4748.

(45) Nguyen, K. A.; Pachter, R. *J. Phys. Chem. A* **2000**, *104*, 4549.

(46) Kajanus, J.; van Berlekom, S. B.; Albinsson, B.; Mårtensson, J. *Synthesis* **1999**, 1155.

(47) Kilså, K.; Kajanus, J.; Mårtensson, J.; Albinsson, B. *J. Phys. Chem. B* **1999**, *103*, 7329.

(48) Bonneau, R.; Wirz, J.; Zuberbühler, A. D. *Pure Appl. Chem.* **1997**, *69*, 979.

(49) Frisch, M. J.; Trucks, G. W.; Schlegel, H. B.; Scuseria, G. E.; Robb, M. A.; Cheeseman, J. R.; Zakrzewski, V. G.; Montgomery, J. A.; Stratmann, R. E.; Burant, J. C.; Dapprich, S.; Millam, J. M.; Daniels, A. D.; Kudin, K. N.; Strain, M. C.; Farkas, O.; Tomasi, J.; Barone, V.; Cossi, M.; Cammi, R.; Mennucci, B.; Pomelli, C.; Adamo, C.; Clifford, S.; Ochterski, J.; Petersson, G. A.; Ayala, P. Y.; Cui, Q.; Morokuma, K.; Malick, D. K.; Rabuck, A. D.; Raghavachari, K.; Foresman, J. B.; Cioslowski, J.; Ortiz, J. V.; Stefanov, B. B.; Liu, G.; Liashenko, A.; Piskorz, P.; Komaromi, I.; Gomperts, R.; Martin, R. L.; Fox, D. J.; Keith, T.; Al-Laham, M. A.; Peng, C. Y.; Nanayakkara, A.; Gonzalez, C.; Challacombe, M.; Gill, P. M. W.; Jahnson, B. G.; Chen, W.; Wong, M. W.; Andres, J. L.; Head-Gordon, M.; Replogle, E. S.; Pople, J. A. *Gaussian 98*, Revision A.9; Gaussian, Inc: Pittsburgh, PA, 1998.

(50) Becke, A. D. *J. Chem. Phys.* **1993**, *98*, 5648.

(51) Ditchfield, R.; Hehre, W. J.; Pople, J. A. *J. Chem. Phys.* **1971**, *54*, 724.

(52) Hehre, W. J.; Ditchfield, R.; Pople, J. A. *J. Chem. Phys.* **1972**, *56*, 2257.

(53) Stratmann, R. E.; Scuseria, G. E.; Frisch, M. J. *J. Chem. Phys.* **1998**, *109*, 8218.

(54) Andréasson, J.; Kajanus, J.; Mårtensson, J.; Albinsson, B. *J. Am. Chem. Soc.* **2000**, *122*, 9844.

(55) Andréasson, J.; Kyrychenko, A.; Mårtensson, J.; Albinsson, B. *Photochem. Photobiol. Sci.* **2002**, *1*, 111.

(56) Lauher, J. W.; Ibers, J. A. *J. Am. Chem. Soc.* **1973**, *95*, 5148.

(57) Silvers, S. J.; Tulinsky, A. *J. Am. Chem. Soc.* **1967**, *89*, 3331.

(58) Hamor, M. J.; Hamor, T. A.; Hoard, J. L. *J. Am. Chem. Soc.* **1964**, *86*, 1938.

(59) Radziszewski, J. G.; Nepras, M.; Balaji, V.; Waluk, J.; Vogel, E.; Michl, J. *J. Phys. Chem.* **1995**, *99*, 14254.

(60) Gouterman, M. *J. Mol. Spectrosc.* **1961**, *6*, 138.

(61) Spellane, P. J.; Gouterman, M.; Kim, A. S.; Liu, Y. C. *Inorg. Chem.* **1980**, *19*, 386.

(62) Sekino, H.; Kobayashi, H. *J. Chem. Phys.* **1987**, *86*, 5045.

(63) Langhoff, S. R.; Davidson, E. R.; Gouterman, M.; Leenstra, W. R.; Kwiram, A. L. *J. Chem. Phys.* **1975**, *62*, 169.

(64) The out-of-plane distortions of the β-carbons are about ± 0.6 and ± 0.45 Å for **ZnDPOMP** and **H₂DPOMP**, respectively.

(65) Bersuker, I. B. *Chem. Rev.* **2001**, *101*, 1067.

(66) Hu, S.; Lin, C.-Y.; Blackwood, M. E.; Mukherjee, A., Jr.; Spiro, T. G. *J. Phys. Chem.* **1995**, *99*, 9694.

(67) Seth, J.; Bocian, D. F. *J. Am. Chem. Soc.* **1994**, *116*, 143.

(68) Angiolillo, P. J.; Lin, V. S.-Y.; Vanderkooi, J. M.; Therien, M. J. *J. Am. Chem. Soc.* **1995**, *117*, 12514.

(69) Wu, G.-Z.; Gan, W.-X.; Leung, H.-K. *J. Chem. Soc., Faraday Trans.* **1991**, *87*, 2933.